Science, accepted for publication 31 March 2021.

Please see journal for version of record

Title: The human dimension of biodiversity changes on islands

Authors: *Sandra Nogué[1*†], Ana M. C. Santos[2,3,4,5], H. John B. Birks[6,7], Svante Björck[8], Alvaro Castilla-Beltrán[1], Simon Connor[9,10], Erik J. de Boer[11], Lea de Nascimento[12,13], Vivian A. Felde[6], José María Fernández-Palacios[12], Cynthia A. Froyd[14], Simon G. Haberle[9,10], Henry Hooghiemstra[15], Karl Ljung[8], Sietze J. Norder[16], Josep Peñuelas[17,18], Matthew Prebble[9,19] Janelle Stevenson[9,10], Robert J. Whittaker[20,21], Kathy J. Willis[22], Janet M. Wilmshurst[13,23], Manuel J. Steinbauer[24,25*†]*

Affiliations:

[1]School of Geography and Environmental Science, University of Southampton, Highfield, SO17 1BJ Southampton, United Kingdom.

[2]cE3c – Centre for Ecology, Evolution and Environmental Changes, Faculdade de Ciências, Universidade de Lisboa, Lisboa, Portugal/Azores Biodiversity Group and Universidade dos Açores, Angra do Heroísmo, Azores, Portugal.

[3]GloCEE - Global Change Ecology and Evolution Group, Department of Life Sciences, Universidad de Alcalá, 28805 Alcalá de Henares, Madrid, Spain.

[4]Terrestrial Ecology Group (TEG), Departamento de Ecología, Universidad Autónoma de Madrid, Madrid, Spain.

[5]Centro de Investigación en Biodiversidad y Cambio Global (CIBC-UAM), Universidad Autónoma de Madrid, Madrid, Spain.

[6]Department of Biological Sciences and Bjerknes Centre for Climate Research, University of Bergen, PO Box 7803, N-5020 Bergen, Norway.

[7]Environmental Change Research Centre, University College London, Gower Street, WC1E 6BT London, United Kingdom.

[8]Department of Geology, Lund University, SE-223 62 Lund, Sweden.

[9]School of Culture, History & Language, College of Asia and the Pacific, Australian National University, ACT 2601, Australia.

[10]ARC Centre of Excellence for Australian Biodiversity and Heritage, Australian National University, ACT 2601, Australia.

[11]Departament d'Estratigrafia, Paleontologia i Geociències Marines, Facultat de Ciències de la Terra, Universitat de Barcelona, Martí i Franquès s/n, 08028 Barcelona, Catalonia, Spain

[12]Island Ecology and Biogeography Group, Instituto Universitario de Enfermedades Tropicales y Salud Pública de Canarias (IUETSPC), Universidad de La Laguna (ULL), 38200 La Laguna, Canary Islands, Spain.

[13]Long-term Ecology Laboratory, Manaaki Whenua – Landcare Research, 7640 Lincoln, New Zealand.

[14]Department of Biosciences, Swansea University, Singleton Park, SA2 8PP Swansea, United Kingdom.

[15]Department of Ecosystem and Landscape Dynamics, Institute of Biodiversity and Ecosystem Dynamics (IBED), University of Amsterdam, Science Park 904, 1098XH Amsterdam, Netherlands.

[16]Leiden University Centre for Linguistics. PO Box 9515, 2300 RA Leiden, Netherlands.

[17]CSIC, Global Ecology Unit, CREAF-CSIC-UAB, Bellaterra, 08193 Barcelona, Catalonia, Spain.

[18]CREAF, Cerdanyola del Vallès, 08193 Barcelona, Catalonia, Spain

[19]School of Earth & Environment, College of Science, University of Canterbury, Christchurch 8140, New Zealand.

[20]School of Geography and the Environment, University of Oxford, OX1 3QY Oxford, United Kingdom.

[21]Center for Macroecology, Evolution and Climate, GLOBE Institute, University of Copenhagen, University of Copenhagen, Universitetsparken 15, Copenhagen 2100, Denmark.

[22]Oxford Long-Term Ecology Laboratory, Department of Zoology, University of Oxford, OX1 3PS Oxford, United Kingdom.

[23]School of Environment, University of Auckland, 1142 Auckland, New Zealand.

[24]Bayreuth Center of Ecology and Environmental Research (BayCEER) & Department of Sport Science, University of Bayreuth, 95447 Bayreuth, Germany.

[25]Department of Biological Sciences, University of Bergen, PO Box 7803, N-5020 Bergen, Norway

*Correspondence to: s.nogue-bosch@soton.ac.uk, steinbauer@uni-bayreuth.de

† Equal contribution.

Abstract: Islands are among the last regions on Earth settled and transformed by human activities and provide replicated model systems for analysis of how people affect ecological functions. By analyzing 27 representative fossil pollen sequences encompassing the past 5000 years from islands globally, we quantify rates of vegetation compositional change before and after human arrival. Following human arrival, rates of turnover accelerate by a median factor of nine, with faster rates on islands colonized in the past 1500 years than for those colonized earlier. This global anthropogenic acceleration in turnover suggests that islands are on trajectories of continuing change. Strategies for biodiversity conservation and ecosystem restoration must acknowledge the long duration of human impacts and the degree to which ecological changes today differ from pre-human dynamics.

One Sentence Summary: Accelerated rates of vegetation turnover in island ecosystems follow initial human settlement around the world

Main Text:

Globally, human activities dominate ecological systems (*1*, *2*) and are considered the main drivers for accelerating contemporary ecosystem transformation (*3-6*). The pressing need to evaluate the extent and dimensions of human impacts as well as the desire to restore 'wild' systems have sparked controversy concerning the value of establishing pre-human baselines (*7-9*) and on the nature and timing of the onset of the Anthropocene (*10-12*). Archaeological and other paleodata on human impacts in continental systems reveal an increasingly human-transformed planet intensifying around the end of the Pleistocene (*2,13,14*). The lengthy time frame of human modification of ecosystem dynamics in continental contexts, spanning periods of substantial post-glacial climate change, complicates the definition of pre-human baselines and hinders the investigation of natural ecosystem processes (*15,16*).

In contrast to continents, most remote oceanic islands were colonized by people relatively recently, within the past three thousand years, when climates were similar to present conditions (*17*). The recent nature of human settlement means that the archaeological, paleoecological, and climate records are often more precisely resolved on well-studied islands compared with continents, and potentially more relevant for understanding remnant ecosystems and informing conservation and ecosystem restoration agendas. Hence, island ecosystems provide opportunities to quantify the critical ecological transition from pre-human to human-dominated ecosystems (*4, 15*), and allow anthropogenic impacts on ecosystems to be placed within the context of long-term pre-human ecological dynamics (*16-20*). While numerous studies have documented the timing, waves, and processes of species extinctions that accompanied human arrival on islands (*18-24*), paleoecological data networks now allow systematic quantification of ecosystem transformations on islands globally. Here, we analyze fossil pollen time-series for multiple independent islands from all the major archipelagos and oceans and across latitudes, using a breakpoint regression approach to test for altered rates and directionality of pollen and hence vegetation compositional turnover connected with human colonization (*25*) within an overall timeframe of the past 5000 years. These time-series of millennial-scale dynamics allow the assessment of whether the rates of vegetation compositional change consistently accelerated across multiple islands following initial

human arrival. Our method employs ordination analyses to characterize the major gradient of compositional variation in the pollen data for each island, quantifying the mean rate of change through time pre- and post-human arrival (Fig. 1), thereby allowing us to assess how human populations impacted islands differently from natural perturbations (*23*).

Our results show that human arrival systematically accelerated directional compositional change in island ecosystems (Figs. 1 and 2). Rates of pollen compositional turnover increase following human arrival by up to a factor of nine, with large differences amongst islands (i.e. a median of 8.9 times higher turnover after human arrival, with a mean of 20.7 ±26.7 times higher turnover). This acceleration is a globally consistent pattern observed on 24 out of 27 islands, independent of current and past island area, latitude, isolation, and elevation of the sampling site (Fig. 3B-3G; Tables S3, S4; *25*). Islands that were settled more recently, such as Poor Knights (13^{th} century)(*19*) and the Galápagos Islands (16^{th} century)(*26*), show a steeper increase in the rate of turnover change (p=0.01, R^2: 0.25; linear regression with log-transformed (arrival time), Fig. 3A) than on islands where humans arrived >1500 years ago (e.g. New Caledonia (*27*) and Fiji (*28*)). This indicates either that the islands settled earlier were more resilient to human arrival or more likely that the recent major compositional turnover observed is explained by introduced species, land-use practices, and technology deployed by later settlers being more transformative than those of earlier settlers. In addition, those islands colonized >3000 years ago appear to show some declines in rates of compositional turnover towards the end of the sequence, although there are too few cases (n=5) to draw firm conclusions.

For many islands, the model implementing a prescribed breakpoint at the time of human arrival closely fits the observed patterns in compositional turnover (Fig. 1). Human arrival estimates fall within the 95% confidence intervals of the optimal breakpoints (representing the greatest change in turnover in each record) for 41% of islands. Human arrival times are within 500 years of the optimal breakpoint for 63% of islands and within 1000 years for 78% of islands (median 338 years compared to 953 for randomized data simulations, Table S5 and Fig. 2). There is no tendency for optimized breakpoints to be systematically earlier or later than estimated human arrival time (t-test with null model of mean difference being 0, p=0.17). A systematic difference would have either indicated earlier human arrival or delayed human impact. On some islands, initial human arrival is not associated with a major shift in turnover (see *25* and Figs. 1 and S1). These results might reflect

the specific local characteristics of the study site. For example, on La Gomera (Canary Islands), the sedimentary sequence was collected at an elevation of 1250 m above sea level (asl) in one of the largest remnant areas of laurel forest, where paleoecological analyses showed no evidence of human impacts (*29*). On other islands, e.g. Hispaniola, shifts in vegetation turnover differ from the time of human arrival that we estimated based on archaeological or historical sources, but the rate of directional change increases (Fig. 1).

Our analysis also shows that ecological change is an integral part of island systems, with changes observed both before recorded human arrivals (median turnover 1.7×10^{-2} [SD_{ptt}/100 years] and mean $4.1 \pm 6.7 \times 10^{-2}$ [SD_{ptt}/100 years]; directional change in composition measured in standard deviations of pollen taxon turnover (SD_{ptt}) per 100 years) and after human arrival (median turnover 14.4×10^{-2} [SD_{ptt}/100 years] and mean $23.1 \pm 30.0 \times 10^{-2}$ [SD_{ptt}/100 years]) (Fig. 2). Results show that the rate of directional turnover prior to human arrival was slower, in contrast to human agencies of change. Natural drivers of ecosystem change on islands, operating before and alongside humans include: volcanic activities, fire, climate change (episodes such as the 'Little Ice Age'), earthquakes, extreme weather events (e.g. droughts and cyclones), and sea-level fluctuations (*20, 30, 31*). While not measurable with the precision to include formally within our analysis, volcanic activities and natural climate fluctuations have likely not increased over the analyzed timeframe across the islands studied and thus cannot explain the systematic increase and varied timing of directional turnover observable across islands (*25*). Climate warming in the last 50 years, in contrast, is too recent to be detectable within our dataset. Over the timeframe of the last five thousand years, direct human impacts greatly outweigh other processes that have shaped island biodiversity and species interactions (*32, 33*).

Moreover, ecological legacies of human arrival on islands may persist for centuries and are often irreversible. An example is Tawhiti Rahi in the Poor Knights archipelago, New Zealand, which is currently uninhabited (*19*). Immediately following initial arrival by Polynesians in the 13th century, the island's forest cover was cleared by fire for human habitation and gardens. After a massacre of local Ngatiwai inhabitants on Tawhiti Rahi in 1820, local *kaitiaki* (guardians) declared the islands *wahi tapu* (protected by a sacred covenant), after which time there was no subsequent settlement. Despite the island becoming totally reforested within 150 years, the current forest composition is completely different to that of the pre-human period. In contrast to the Poor Knights archipelago,

most currently inhabited islands have experienced at least two distinct waves of settlement, each with distinctive signatures of change and leaving increasingly complex legacies (*24*,*30*).

Preparing and managing for ecosystem change is one of the major challenges that island societies currently face as islands experience continued or accelerated threats from detrimental land-use practices (*12*), novel species invasions (*24, 34*), sea-level rise (*35*), and climate change (*11, 17*) in addition to naturally occurring disturbances. The challenges are made more difficult as these processes are affecting native ecosystems where vegetation communities have already been severely degraded or lost, species have gone extinct (*15, 21*), and important mutualistic plant–animal interactions have been disrupted (*36*). Our results show little indication that these human-impacted ecosystems are either similar to, or returning to, the dynamic baselines observed prior to human arrival. Hence, anthropogenic impacts on islands are lasting components of these systems, typically involving initial clearance (e.g. using fire), and then compounded by the introduction of a range of introduced species and extinctions of endemic species and ongoing disturbances. This contrasts with turnover following natural disturbances in the pre-human period, when island ecosystems often recovered rapidly to pre-disturbance states (e.g, *20, 31*). While for many islands, widescale return to pre-colonization ecosystems is an unrealistic goal, paleoecological data, such as analyzed here, may serve to inform targeted ecosystem restoration efforts within islands, providing insights into previous system states and their responsiveness to global change processes (*9, 37*).

Reference and Notes:

1. P. M. Vitousek, H. A. Mooney, J. Lubchenco, J. M. Melillo, Human domination of Earth's ecosystems. *Science* **277**, 7 (1997).

2. L. Stephens, D. Fuller, N. Boivin, T. Rick, N. Gauthier, A. Kay, *et al*., Archaeological assessment reveals Earth's early transformation through land use. *Science* **365**, 897–902 (2019).

3. S. E. Connor, J. F. N. van Leeuwen, T. M. Rittenour, W. O. van der Knaap, B. Ammann, S. Björck, The ecological impact of oceanic island colonization – a palaeoecological perspective from the Azores. *J. Biogeogr.* **39**, 1007–1023 (2012).

4. S. Nogué, L. de Nascimento, C. A. Froyd, J. M. Wilmshurst, E. J. de Boer, E. E. D. Coffey, *et al*. Island biodiversity conservation needs palaeoecology. *Nat. Ecol. Evol.* **1**, 0181 (2017).

5. W. Steffen, W. Broadgate, L. Deutsch, O. Gaffney, C. Ludwig, The trajectory of the Anthropocene: The great acceleration. *Anthropocene Rev.* **2**, 81–98 (2015).

6. M. J. Steinbauer, J.-A. Grytnes, G. Jurasinski, A. Kulonen, J. Lenoir, H. Pauli, *et al*., Accelerated increase in plant species richness on mountain summits is linked to warming. *Nature* **556**, 231–234 (2018).

7. K. J. Willis, R. M. Bailey, S. A. Bhagwat, H. J. B. Birks, Biodiversity baselines, thresholds and resilience: testing predictions and assumptions using palaeoecological data. *Trends Ecol. Evol.* **25**, 583–591 (2010).

8. R. J. Hobbs, S. Arico, J. Aronson, J. S. Baron, P. Bridgewater, V. A. Cramer, *et al*., Novel ecosystems: theoretical and management aspects of the new ecological world order. *Global Ecol. Biogeogr.* **15**, 1–7 (2006).

9. A.D. Barnosky, E. A. Hadly, P. Gonzalez, J. Head, P. D. Polly, P. D., A. M Lawing, *et al.*, Merging paleobiology with conservation biology to guide the future of terrestrial ecosystems. *Science* **355**, 6325 (2017).

10. W. F. Ruddiman, Three flaws in defining a formal 'Anthropocene'. *Prog. Phys. Geog*. **42**, 451–461 (2018).

11. J. Zalasiewicz, C. N. Waters, M. J. Head, C. Poirier, C. P. Summerhayes, R. Leinfelder, J. *et al*., A formal Anthropocene is compatible with but distinct from its diachronous anthropogenic counterparts: a response to W.F. Ruddiman's 'three flaws in defining a formal Anthropocene'. *Prog. Phys. Geog.* 4**3**, 319–333 (2019).

12. C. S. M. Turney, J. Palmer, M. A. Maslin, A. Hogg, C. J. Fogwill, J. Southon, *et al*., Global peak in atmospheric radiocarbon provides a potential definition for the onset of the Anthropocene Epoch in 1965. *Sci. Rep.* **8**, 3293 (2018).

13. E. C. Ellis, D. Q. Fuller, J. O. Kaplan, W. G. Lutters, Dating the Anthropocene: Towards an empirical global history of human transformation of the terrestrial biosphere. *Elementa: Science of the Anthropocene*. **1** (2013), doi:10.12952/journal.elementa.000018.

14. Y. Malhi, C. E. Doughty, M. Galetti, F. A. Smith, J.-C. Svenning, J. W. Terborgh, Megafauna and ecosystem function from the Pleistocene to the Anthropocene. *Proc Natl Acad Sci USA.* **113**, 838 (2016).

15. H. J. B. Birks, Contributions of Quaternary botany to modern ecology and biogeography. *Plant. Ecol. Divers.* **12**, 189–385 (2019).

16. J. R. Wood, G. L. W. Perry, J. M. Wilmshurst, Using palaeoecology to determine baseline ecological requirements and interaction networks for de-extinction candidate species. *Funct. Ecol.* **31**, 1012–1020 (2017).

17. C. Nolan, J. T. Overpeck, J. R. M. Allen, P. M. Anderson, J. L. Betancourt, H. A. Binney, S. *et al.*. Past and future global transformation of terrestrial ecosystems under climate change. *Science* **361**, 920–923 (2018).

18. W. D. Gosling, D. A. Sear, J. D. Hassall, P. G. Langdon, M. N. T. Bönnen, T. D. Driessen, *et al*. Human occupation and ecosystem change on Upolu (Samoa) during the Holocene. *J. Biogeogr.* **47**, 600–614 (2020).

19. J. M. Wilmshurst, N. T. Moar, J. R. Wood, P. J. Bellingham, A. M. Findlater, J. J. Robinson, C. Stone, Use of pollen and ancient DNA as conservation baselines for offshore islands in New Zealand. *Conserv. Biol.* **28**, 202–212 (2014).

20. J. M. Wilmshurst, M. S. McGlone, T. R. Partridge, A late Holocene history of natural disturbance in lowland podocarp/hardwood forest, Hawke's Bay, New Zealand. *N. Z. J. Bot.* **35**, 79–96 (1997).

21. D.W. Steadman, Prehistoric extinctions of Pacific Islands birds: Biodiversity meets Zooarchaeology. *Science* **267**, 1123–1131 (1995).

22. D. A. Burney, T. F. Flannery, Fifty millennia of catastrophic extinctions after human contact. *Trends Ecol. Evol.* **20**, 395–401 (2005).

23. R. J. Whittaker, J. M. Fernández-Palacios, *Island Biogeography: Ecology, Evolution, and Conservation* (Oxford Univ. Press, 2007).

24. J. R. Wood, J. A. Alcover, T. M. Blackburn, P. Bover, R. P. Duncan, J. P. Hume, *et al*., Island extinctions: processes, patterns, and potential for ecosystem restoration. *Environ. Conserv.* **44**, 348–358 (2017).

25. Materials and methods are available as supplementary materials at the Science website.

26. A. Restrepo, P. Colinvaux, M. Bush, A. Correa-Metrio, J. Conroy, M. R. Gardener, P. Jaramillo, M. Steinitz-Kannan, J. Overpeck, Impacts of climate variability and human colonization on the vegetation of the Galápagos Islands. *Ecology* **93**,1853–1866 (2012).

27. J. Stevenson, R. Dodson, I. P. Prosser, A late Quaternary record of environmental change and human impact from Plum Swamp, New Caledonia. *Palaeogeogr. Palaeoclimatol. Palaeoecol.* **168**, 97–123 (2001).

28. G. Hope, J. Stevenson, W. Southern, Vegetation histories from the Fijian Islands: Alternative records of human impact, in G. Clark, Ed. The early prehistory of Fiji. *Terra Australis* **31** (ANU ePress, Canberra, ACT, Australia, 2009), pp. 63–86.

29. S. Nogué, L. de Nascimento, J. M. Fernández-Palacios, R. J. Whittaker, K. J. Willis, The ancient forests of La Gomera, Canary Islands, and their sensitivity to environmental change. *J. Ecol.* **101**, 368–377 (2013).

30. B. Rolett, J. Diamond, Environmental predictors of pre-European deforestation on Pacific islands. *Nature* **431**, 443–446 (2004).

31. J. M. Wilmshurst, M. S. McGlone, Forest disturbance in the central North Island, New Zealand, following the. 1850 BP Taupo eruption. *The Holocene* **6,** 399-411 (1996).

32. M. R. Helmus, D. L. Mahler, J. B. Losos, Island biogeography of the Anthropocene. *Nature* **513**, 543–546 (2014).

33. H. Kreft, W. Jetz, J. Mutke, G. Kier, W. Barthlott, Global diversity of island floras from a macroecological perspective. *Ecol. Lett.* **11**, 116–127 (2008).

34. D. Moser, B. Lenzner, P. Weigelt, W. Dawson, H. Kreft, J. Pergl, *et al*., Remoteness promotes biological invasions on islands worldwide. *Proc. Natl. Acad. Sci. U.S.A.* **115**, 9270 (2018).

35. S. J. Norder, J. B. Baumgartner, P. A. V. Borges, *et al.*, A global spatially explicit database of changes in island palaeo-area and archipelago configuration during the late Quaternary. *Global Ecol. Biogeogr.* **27**, 500– 505 (2018).

36. C. N. Kaiser-Bunbury, A. Traveset, D. M. Hansen, Conservation and restoration of plant–animal mutualisms on oceanic islands. *Perspect. Plant Ecol. Evol. Syst.* **12**, 131–143 (2010).

37. J.-C. Svenning, Proactive conservation and restoration of botanical diversity in the Anthropocene's "rambunctious garden". *Am. J. Bot.* **105**(6), 963–966 (2018).

38. S. Goring, A. Dawson, G. L. Simpson, K. Ram, R. W. Graham, E. C. Grimm, J. W. Williams, Neotoma: a programmatic interface to the Neotoma palaeoecological database. *Open Quat.* **1**, art.2 (2015).

39. J. Haslett, A.C. Parnell, A simple monotone process with application to radiocarbon-dated depth chronologies. *J. R. Stat. Soc. Ser. C Appl. Stat*. **57**, 399-41 (2008).

40. A. C. Parnell, J. Haslett, J. R. M. Allen, C.E. Buck, B. Huntley, A flexible approach to assessing synchroneity of past events using Bayesian reconstructions of sedimentation history. *Quat. Sci. Rev.* **27**1872–1885 (2008).

41. J. Van der Plicht, C. Bronk Ramsey, T. Heaton, E. Scott, S. Talamo, Recent developments in calibration for archaeological and environmental samples. *Radiocarbon* 1–23. (2020).

42. M. Blaauw, clam: Classical Age-Depth Modelling of Cores from Deposits. R package version 2.3.5. (2020). (available at CRAN.R-project.org/package=clam).

43. R Core Team, R: A language and environment for statistical computing. *R Foundation for Statistical Computing*, Vienna, Austria (2019) (available at www.R-project.org).

44. J. Oksanen, F. G. Blanchet, M. Friendly, R. Kindt, P. Legendre, D. McGlinn, P. R. Minchin, R. B. O'Hara, G. L. Simpson, P. Solymos, M. H. H. Stevens, E. Szoecs, H. Wagner, vegan: *Community Ecology Package* (2019) (available at CRAN.R-project.org/package=vegan).

45. M. O. Hill, H. G. Gauch, Detrended correspondence analysis: an improved ordination technique, In E. van der Maarel, Ed. Classification and Ordination. *Advances in Vegetation Science*, vol. 2. (Springer, Dordrecht, 1980).

46. P. Breheny, W. Burchett, Visualization of regression models using visreg. *The R Journal* **9**, 56 (2017).

47. V.M.R. Muggeo. Interval estimation for the breakpoint in segmented regression: a smoothed score-based approach. *Aust N Z J Stat* **59**, 311-322 (2017).
48. L. Anderson, D.B Wahl, T. Bhattacharya, Understanding rates of change: a case study using fossil pollen records from California to assess the potential for and challenges to a regional data synthesis. *Quat. Int.* https://doi.org,/10.1016/jquaint.2020.04.044/(2020).

49. E.C. Grimm, G.L, Jacobson, 1992. Fossil-pollen evidence for abrupt climate changes during the past 18000 years in eastern North America. *Clim. Dyn.* **6**, 179–184 (1992).

50. C.J.F. Ter Braak, P. Šmilauer, *Canoco reference manual and user's guide: software for ordination (version 5)*. Microcomputer Power, Ithaca, New York, (2012).

51. J. Braje, J. M. Erlandson, Human acceleration of animal and plant extinctions: A Late Pleistocene, Holocene, and Anthropocene continuum. *The Anthropocene* **4**, 14-23 (2013).

52. D. W. Steadman, Extinction & biogeography of tropical Pacific birds. (University of Chicago Press, 2007).

53. H. Kreft, W. Jetz, Global patterns and determinants of vascular plant diversity. *Proc. Natl. Acad. Sci. U.S.A.* **104**, 5925–5930 (2007).

54. A. H. Harcourt, *Human Biogeography* (1st ed.). (University of California Press, JSTOR, 2012).

55. S. J. Norder, R. F. de Lima, L. de Nascimento, J. Y. Lim, J. M. Fernández-Palacios, M.M. Romeiras, R. B. Elias, *et al.*, Global change in microcosms: Environmental and societal predictors of land cover change on the Atlantic Ocean Islands, *Anthropocene* **30**, 2213–3054 (2020).

56. A. Chiarucci, S. Fattorini, B. Foggi, L. Sara, L. Lazzaro, J. Podani *et al*, Plant recording across two centuries reveals dramatic changes in species diversity of a Mediterranean archipelago. *Sci. Rep.* **7**, 5415 (2017).

57. R. H. MacArthur, E.O. Wilson, *The theory of island biogeography* (1st ed.). (Princeton University Press 1967).

58. S. J. Norder, K. Proios, R. J. Whittaker, M. R. Alonso, P. A. V. Borges, M. K. Borregaard, *et al.*, Beyond the Last Glacial Maximum: Island endemism is best explained by long-lasting archipelago configurations. *Global Ecol. Biogeogr*. **28**, 184–197. (2019).

59. P. Weigelt, H. Kreft, Quantifying island isolation – Insights from global patterns of insular plant species richness. *Ecography* **36**, 417–429 (2013).

60. S. J. Wright, How isolation affects rates of turnover of species on islands. *Oikos* **44**(2), 331-340 (1985).

61. H. Shaefer, *Flora of the Azores* (2nd edition). (Margraf Publishers, Weikersheim, 2005).

62. V. Rull, A. Lara, M. J. Rubio-Inglés, S. Giralt, V. Gonçalves, P. Raposeiro, *et al.*, Vegetation and landscape dynamics under natural and anthropogenic forcing on the Azores Islands: A 700-year pollen record from the São Miguel Island. *Quat. Sci. Rev.* **159**, 155–168 (2017).

63. K. D. Patterson, Epidemics, famines, and population in the Cape Verde Islands, 1580-1900. *Int. J. Afr. Hist. Stud.* **21**, 291–313 (1988).

64. J.Velasco, V, Alberto, T. Delgado, M. Moreno, C. Lecuyer, P. Richardin, P, Poblamiento, colonización y primera historia de Canarias: el C14 como paradigma. *Anu. Estud. Atl.* **66**, 1e24 (2019).

65. L. de Nascimento, S.Nogué, A.Naranjo-Cigala, C. Criado, M. McGlone, E. Fernández-Palacios, *et al.*, Human impact and ecological changes during prehistoric settlement on the Canary Islands, *Quat. Sci. Rev*. **239**, 106332 (2020).

66. M. Arnay-de-la-Rosa, A. Gámez-Mendoza, J. F. Navarro-Mederos, J. C. Hernández-Marrero, R. Fregel, Y. Yanes, L. Galindo-Martín, C.S. Romanek, E. González-Reimers, Dietary patterns during the early prehispanic settlement in La Gomera (Canary Islands). *J. Arch. Sci*. **36**, 1972–1981 (2009).

67. J. C. Rando, J. A. Alcover, B. Galván, J. F. Navarro, Reappraisal of the extinction of *Canariomys bravoi*, the giant rat from Tenerife (Canary Islands). *Quat. Sci. Rev.* **94**, 22–27 (2014).

68. S. B. Cooke, L. M. Dávalos, A. M. Mychajliw, S. T. Turvey, N. S. Upham, Anthropogenic extinction dominates Holocene declines of West Indian mammals. *Annu. Rev. Ecol. Evol. Syst.* **48**, 301–327 (2017).

69. J. K. Headland, *Chronological list of Antarctic expeditions and related historical events.* (Cambridge University Press, Cambridge, 1989).

70. M. Halsdóttir, Pollen analytical studies of human influence on vegetation in relation to the Landnám tephra layer in southwest Iceland. Lundqua Thesis, 18, 45 pp (1987).

71. A. Cheke, J. P. Hume, *Lost land of the dodo. An ecological history of the Mascarene Islands.* (Bloomsbury, 2008).

72. T. M. Reith, E. E. Cochrane, The chronology of colonization in remote Oceania, in *The Oxford Handbook of Prehistoric Oceania*, T. L. Hunt, E. E. Cochrane, Eds. (Oxford University Press, Oxford, 2017).

73. F. Petchey, M. Spriggs, F. Leach, M. Seed, C. Sand, M. Pietrusewsky, K. Anderson, Testing the human factor: radiocarbon dating the first peoples of the South Pacific. *J. Arch. Sci*. **38**, 29–44 (2011).

74. P. A. Colinvaux, E. K. Schofield, Historical ecology in the Galápagos Islands, Holocene pollen record from El Junco Lake, Isla San Cristobal. *J. Ecol.* **64**, 989–1012 (1976).

75. C. A. Froyd, J. A. Lee, A. J. Anderson, S. G. Haberle, P. E. Gasson, K. J. Willis, Historic fuel wood use in the Galápagos Islands: identification of charred remains. *Veget. Hist. Archaeobot*. **19**, 207–217 (2010).

76. T. M. Rieth, T. L. Hunt, C. Lipo, J. M. Wilmshurst, The 13th century Polynesian colonization of Hawai'i Island. *J. Arch. Sci*. **38**, 2740–2749 (2011).

77. A. Anderson, S. Haberle, G. Rojas, A. Seelenfreund, I. Smith, T. Worthy, An archaeological exploration of Robinson Crusoe Island, Juan Fernandez Archipelago, Chile, in *Fifty years in the field*. *Essays in honour and celebration of Richard Shutler Jr's archaeological career*, S. Bedford, C. Sand, D. Burley, Eds. (Auckland: New Zealand Archaeological Association Publications, 2002).

78. J. M. Wilmshurst, A.J. Anderson, T.F.G. Higham, T.H. Worthy, Dating the late prehistoric dispersal of Polynesians to New Zealand using the commensal Pacific rat. *Proc. Natl. Acad. Sci. U.S.A.* **105** (22), 7676–7680 (2008).

79. R. Green, A retrospective view of settlement pattern studies in Samoa. In: *Pacific landscapes. Archaeological approaches*, T. N. Ladefoged, M. W. Graves, Eds. (Los Osos: Easter Island Foundation, Bearsville Press 2002).

80. J. G. Kahn, Y. Sinoto, Refining the Society Islands cultural sequence: Colonization phase and developmental phase coastal occupation on Mo'orea Island. *J. Polynesian Soc.* **126**, 33–60 (2017).

81. J. M. Wilmshurst, T. L. Hunt, C. P. Lipo, A. J. Anderson, High-precision radiocarbon dating shows recent and rapid initial human colonization of East Polynesia. *Proc. Natl. Acad. Sci. U.S.A.* **108**, 1815–1820 (2011).

82. S. Björck, T. Rittenour, P. Rosén, Z. França, P. Möller, I. Snowball, S. Wastegård, O. Bennike, B. Kromer, A Holocene lacustrine record in the central North Atlantic: proxies for volcanic activity, short-term NAO mode variability and long-term precipitation changes. *Quat. Sci. Rev.* **25**, 9–32 (2006).

83. A. Castilla-Beltrán, I. Duarte, L. de Nascimento, J. M. Fernández-Palacios, M. Romeiras, R. J. Whittaker, M. Jambrina-Enríquez, C. Mallol, A. B. Cundy, M. E. Edwards, S. Nogué, Using multiple palaeoecological indicators to guide biodiversity conservation in tropical dry islands: the case of São Nicolau, Cabo Verde. *Biol. Cons.* **242**, 108397 (2020).

84. A. Castilla-Beltrán, L. de Nascimento, J. M. Fernández-Palacios, T. Fonville, R. J. Whittaker, M. E. Edwards, S. Nogué, Late Holocene environmental change and the

anthropization of the highlands of Santo Antão Island, Cabo Verde. *Palaeogeogr. Palaeoclimatol. Palaeoecol.* **524**, 101–117 (2019).

85. L. de Nascimento, S. Nogué, C. Criado, C. Ravazzi, R. J. Whittaker, K. J. Willis, J. M. Fernández-Palacios, Reconstructing Holocene vegetation on the island of Gran Canaria before and after human colonization. *The Holocene* **26**, 113–125 (2016).

86. L. de Nascimento, K. J. Willis, J. M. Fernández-Palacios, C. Criado, R. J. Whittaker, The long-term ecology of the lost forests of La Laguna, Tenerife (Canary Islands). *J. Biogeogr.* **36**, 499–514 (2009).

87. S. D. Crausbay, P. H. Martin, E. F. Kelly, Tropical montane vegetation dynamics near the upper cloud belt strongly associated with a shifting ITCZ and fire. *J. Ecol.* **103**, 891–903 (2015).

88. K. Ljung, S. Björck, Holocene climate and vegetation dynamics on Nightingale Island, South Atlantic – an apparent interglacial bipolar seesaw in action? *Quat. Sci. Rev.* **26,** 3150–3166 (2007).

89. K. Ljung, S. Björck, D. Hammarlund, L. Barnekow, Late Holocene multi-proxy records of environmental change on the South Atlantic island Tristan da Cunha. *Palaeogeogr. Palaeoclimatol. Palaeoecol.* **241**, 539–560 (2006).

90. M. Halsdóttir, Pollen analytical studies of human influence on vegetation in relation to the Landnám tephra layer in southwest Iceland. Lundqua Thesis, 18, 45 pp (1987).

91. E. J. de Boer, H. Hooghiemstra, F. B. Vincent Florens, C. Baider, S. Engels, V. Dakos, M. Blaauw, K. D. Bennett, Rapid succession of plant associations on the small ocean island of Mauritius at the onset of the Holocene. *Quat. Sci. Rev.* **68**, 114–125 (2013).

92. W. Southern, *The Late Quaternary environmental history of Fiji*, PhD Thesis. (Australian National University, Canberra, 1986).

93. G. Hope, J. Stevenson, W. Southern, Vegetation histories from the Fijian Islands: Alternative records of human impact, In: *The early prehistory of Fiji*, G. Clark, Ed. (ANU ePress, Canberra, ACT, Australia, 2009).

94. S. Pau, G. M. MacDonald, T. W. Gillespie, A dynamic history of climate change and human impact on the environment from Keālia Pond, Maui, Hawaiian Islands. *Ann. Am. Assoc. Geogr.* **102**, 748–762 (2012).

95. S. G. Haberle, Late Quaternary vegetation dynamics and human impact on Alexander Selkirk Island, Chile. *J. Biogeogr.* **30**, 239–255 (2003).

96. A. J. Anderson, S. G. Haberle, G. Rojas, A. G. Seelenfreund, I. W. Smith, I. W. T. Worthy, An archaeological exploration of Robinson Crusoe Island, Juan Fernandez Archipelago, Chile, In: *Fifty years in the field: essays in honour and celebration of Richard Shutler Jr's archaeological career*, S. Bedford, C. Sand, D. Burley, Eds. (New Zealand Archaeological Association Monograph 25, 2002).

97. S. G. Haberle, Juan Fernandez Islands, In: *Encyclopedia of Islands*, R. Gillespie, D. A. Clague, Eds. (University of California Press, Berkeley, CA, 2009).

98. S. J. Holdaway, J. Emmitt, L. Furey, A. Jorgensen, G. O'Regan, R. Phillipps, M. Prebble, R. Wallace, T. N. Ladefoged, Māori settlement of New Zealand: The Anthropocene as a process. *Arch. Oceania* **54**, 17–34 (2019).

99. M. Prebble, A. J. Anderson, P. Augustinus, J. Emmitt, S. J. Fallon, L. L. Furey, S. J. Holdaway, A. Jorgensen, T. N. Ladefoged, P. J. Matthews, J. Y. Meyer, R. Phillipps, R. Wallace, N. Porch, Early tropical crop production in marginal subtropical and temperate Polynesia. *Proc. Natl. Acad. Sci. U.S.A.*, 201821732 (2019).

100. J. Stevenson, A. Benson, J. S. Athens, J. Kahn, P. V. Kirch, Polynesian colonization and landscape changes on Mo'orea, French Polynesia: The Lake Temae pollen record. *The Holocene* **27**, 1963–1975 (2017).

101. M. Prebble, J. M. Wilmshurst, Detecting the initial impact of humans and introduced species on island environments in remote Oceania using palaeoecology. *Biol. Inv.* **11**, 1529–1556 (2009).

102. D. Kennett, A. Anderson, M. Prebble, E. Conte, J. Southon, Prehistoric human impacts on Rapa, French Polynesia. *Antiquity* **80**, 340–354 (2006).

103. M. Prebble, A. Anderson, D. J. Kennett, Forest clearance and agricultural expansion on Rapa, Austral Archipelago, French Polynesia. *The Holocene* **23**, 179–196 (2013).

104. D.A. Sear, M.S. Allen, J.D. Hassall, A.E. Maloney, P.G. Langdon, A.E. Morrison. Human settlement of East Polynesia earlier, incremental, and coincident with prolonged South Pacific drought. *Proc. Natl. Acad. Sci. U.S.A.*, **117,** 8813-8819 (2020).

105. J. W. Williams, E.G. Grimm, J. Blois, D.F. Charles, E. Davis, S.J. Goring, *et al.*, The Neotoma Paleoecology Database: A multi-proxy, international community-curated data resource. *Quat. Res.* **89**, 156–177 (2018).

106. R. M. Fyfe, J. L. de Beaulieu, H. Binney, R. H. W. Bradshaw, S. Brewer, A. Le Flao, W. Finsinger, *et al*, The European Pollen Database: past efforts and current activities. *Veg. Hist. Archaeobot.* **18**, 417-424 (2009).

107. P. de Menocal, J. Ortiz, T. Guilderson, J. Adkins, M. Sarnthein, L. Baker, *et al*. Abrupt onset and termination of the African Humid Period: rapid climate responses to gradual insolation forcing. *Quat. Sci. Rev*. **19**, 347–361 (2000).

108. H. Li, A. Sinha, A. Anquetil André, C. Spötl, H. B. Vonhof, A. Meunier, *et al*, A multimillennial climatic context for the megafaunal extinctions in Madagascar and Mascarene Islands. *Sci. Adv.* **6**, eabb2459 (2020).

109. E. J. de Boer, M. I. Vélez, K. F. Rijsdijk, P. G. B. de Louw, T. J. J. Vernimmen, P.M. Visser, R. Tjallangii, H. Hooghiemstra, A deadly cocktail: How a drought around 4200 cal. yr BP caused mass mortality events at the infamous 'dodo swamp' in Mauritius. *The Holocene* **25**, 758-771 (2013)

110. A. G. Hogg, T. F. G. Higham, D. J. Lowe, J. G. Palmer, P. J. Reimer, R. M. Newnham, A wiggle-match date for Polynesian settlement in New Zealand. *Antiquity* **77**, 116-125 (2003).

111. G. F. Camoin, L. Montaggioni, C. Braithwaite, Late glacial to post glacial sea-levels in the Western Indian Ocean. *Mar. Geol.* **206**, 119–146 (2004).

Acknowledgements: Funding: A.M.C.S was supported by a "Juan de la Cierva" Fellowship (IJCI-2014-19502) funded by the Spanish 'Ministerio de Ciencia, Innovación y Universidades', and by the Portuguese "Fundação para a Ciência e a Tecnología" (contract CEEIND/03425/2017). H.J.B.B., V.A.F., and M.J.S. acknowledge support from the European Research Council under the EU H2020 research and innovation programme (grant 741413 HOPE) Humans on Planet Earth – Long-term impacts on biosphere dynamics. J.P. was supported by the European Research Council grant ERC-SyG-2013-610028 IMBALANCE-P. L.dN. was supported by the European Union's Horizon 2020 research and innovation programme under the Marie Skłodowska-Curie grant agreement No 700952. M.J.S was supported by the Deutsche Forschungsgemeinschaft (STE 2360/2-1 embedded in the Research Unit TERSANE FOR 2332). S.B and K.L were supported by several grants from the Swedish Research Council (VR). S.N acknowledges support from the Worldwide Universities Network (WUN) Research Mobility Programme and a generous sabbatical granted by the School of Geography and Environmental Science (University of Southampton). S.J.N gratefully acknowledges support from the European Research Council under the EU H2020 and Research and Innovation programme (grant 818854 SAPPHIRE). **Author contributions:** S.N. and M.J.S. led, analyzed the datasets, and wrote the paper together with all authors: A.M.C.S., H.J.B.B., S.B., A.C.B., J.M.W., S.C., E.J.d.B., L.dN., V.A.F., J.M.F.P., C.A.F., S.G.H., H.H., K.L., S.J.N., J.P., M.P., J.S., R.J.W., K.J.W. All authors contributed in the discussion. **Competing interests:** The authors declare no competing interests**. Data and materials availability:** All datasets will be uploaded to the Neotoma Paleoecology Database when the manuscript is published. Code will be made available in Dryad.

Supplementary Materials:

Fig. 1. Human arrival accelerated compositional turnover on islands. Global analysis of rate of palynological and hence vegetation compositional turnover (slope of the line) for 27 representative fossil pollen records from sedimentary sequences on islands. The x-axis represents calibrated years BP (cal yr BP=years before 1950) calculated using Bayesian age-depth models for each island (*25*). The y-axes represent the major gradient in pollen composition quantified by the ordination axis 1 scores of separate Detrended Correspondence Analyses (DCA) of each sequence. The units are measured in DCA axis scores, which approximate the standard deviation of pollen taxon compositional turnover (SD_{ptt}), with a SD of 4 corresponding roughly to 100% compositional turnover. These plots show results of breakpoint analyses of the rate of compositional turnover with the date of recorded human arrival as the prescribed breakpoint. The recorded date of human arrival is indicated by the vertical orange line (see Table S3 for details). Scaling varies among panels. Shaded areas (blue) depict 95% confidence intervals of the models. A second continuous breakpoint analysis was implemented which detects the major statistical change point in turnover rate intrinsic to the data. This 'optimized breakpoint' is indicated by the vertical dashed black line.

Fig. 2: Rates of turnover before and after human arrival. Change in the rate of pollen compositional turnover before (on the left) and after recorded date of human settlement (purple) for the time-series of fossil pollen records for each of 27 islands, globally, where each island's sequence has been subject to a separate ordination analysis using DCA. Rate of pollen taxon turnover is quantified as the absolute slope in the relationship between ordination scores of the first axis of each DCA with time. The units approximate standard deviation of compositional turnover per 100 years (SD_{ptt}/100 years). The pre-settlement rate of compositional turnover is represented on the left (median: 1.7×10^{-4}; mean: 4.0×10^{-4}) and the rate post-human arrival is represented on the right (median: 14.4×10^{-4}; mean: 23.2×10^{-4}). The difference is highly significant ($p<0.001$; paired *t*-test). See (*21*) for details.

Fig. 3: Differences between the pre-human and human-dominated turnover scale with human-arrival times. Relationships between the change in the rate of pollen compositional turnover pre- and post-human arrival and several island features, showing: a curvilinear decrease in observed turnover as the time elapsed since the first colonization increases (A), but no relationship with Turnover rate before human arrival (B), latitude (C), elevation of the coring site (D), island area (E) glacial-interglacial area (F), and isolation (represented by distance to mainland (G) or surrounding landmass (H)). Asterisks (**) correspond to $p<0.01$ (panel A).

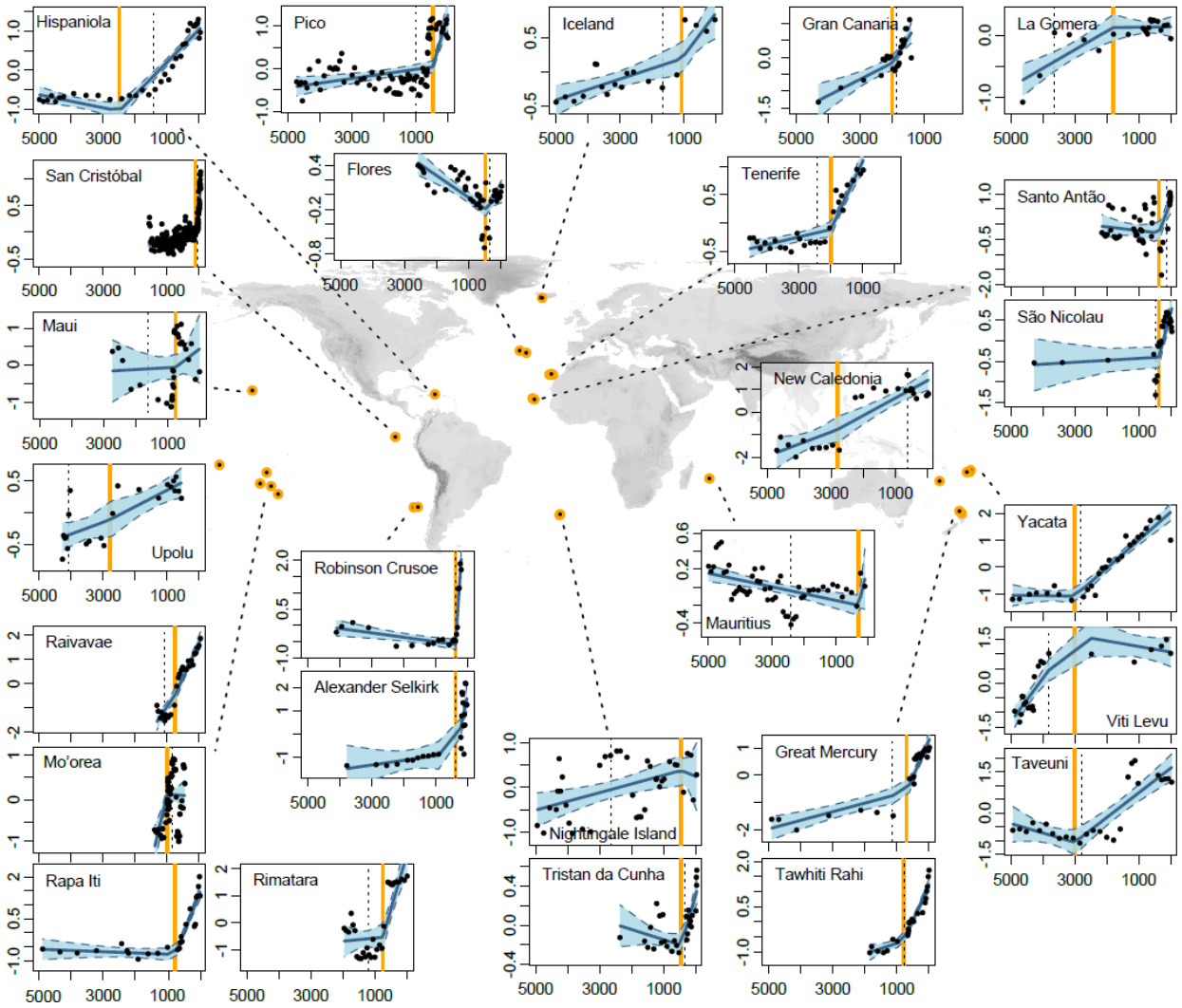
Hispaniola
Pico
Iceland
Gran Canaria
La Gomera
San Cristóbal
Flores
Tenerife
Santo Antão
Maui
São Nicolau
New Caledonia
Upolu
Yacata
Robinson Crusoe
Mauritius
Raivavae
Alexander Selkirk
Viti Levu
Mo'orea
Great Mercury
Taveuni
Nightingale Island
Rapa Iti
Rimatara
Tristan da Cunha
Tawhiti Rahi
5000
3000
1000

Figure 1

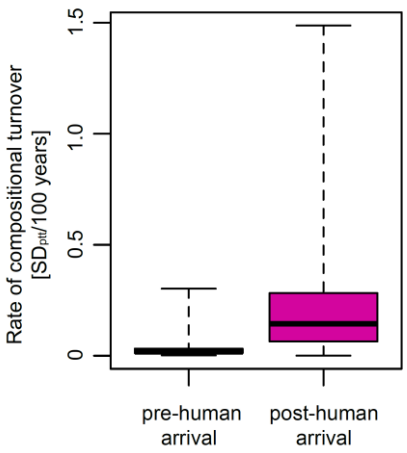

Figure 2

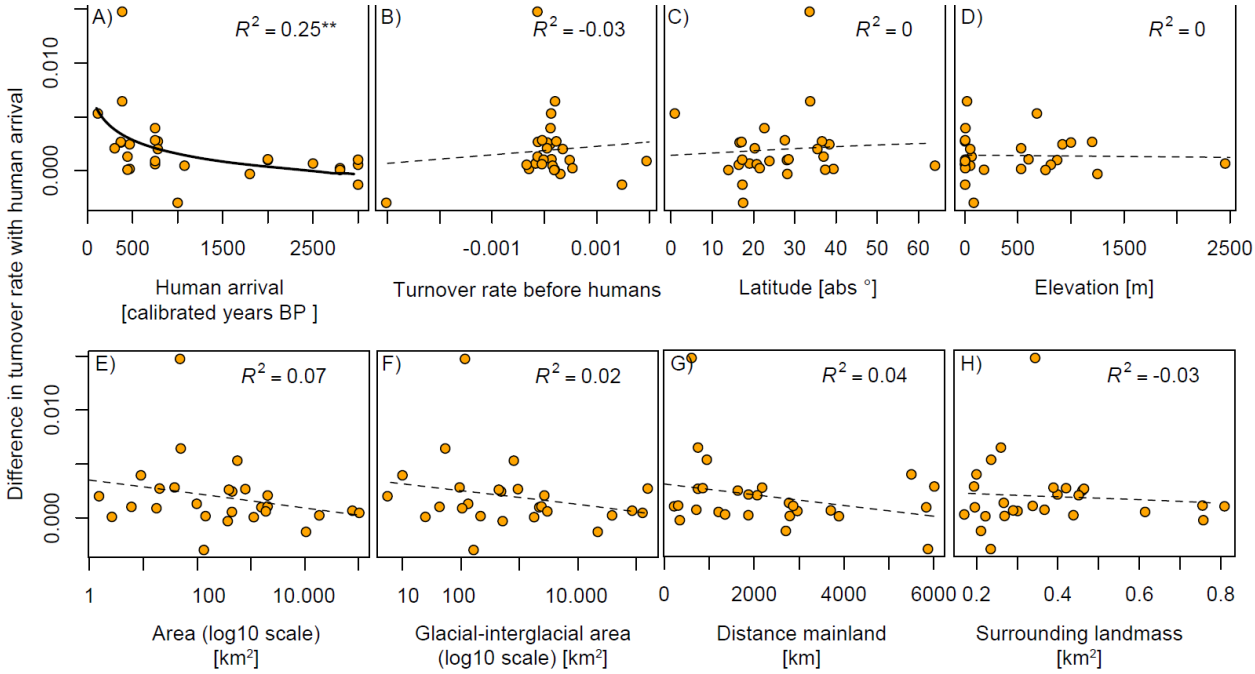

Figure 3

Materials and Methods

Data acquisition and preparation

We analyze fossil pollen time-series in sedimentary sequences from islands on which the initial presence of humans is recoded within the past 5000 years. This time frame allows the assessment of vegetation dynamics in continuous time-series from systems when humans were entirely absent to systems where humans represent a novel disturbance (Table S1). We obtained fossil pollen records from The Neotoma Paleoecology Database (*38*) and the published literature (Table S4). All pollen records that we could obtain covering human arrival on islands are included in the manuscript. To maintain consistency between islands and avoid island redundancy, the pollen record with the highest temporal resolution for our study period was selected whenever more than one dataset was available for an island. To avoid geographic biases, we applied the criteria that no single archipelago should be represented by more than three islands, resulting in data for 27 islands being retained for analysis.

Each pollen dataset was screened to remove obligate aquatic and semi-aquatic taxa (following standard paleoecological methodology) and exotic marker taxa (*Lycopodium* spores or *Eucalyptus* pollen). Pollen taxonomy is site specific and includes both identified and unidentified pollen and spore morphotypes, because they represent plant taxa that contribute to turnover and because we presume that the researchers that obtained the data know best which palynomorphs reflect local vegetation. Pollen taxa are not equivalent to species as identification varies to family, genus, occasionally to species, or to pollen types. Hence our analyses are based on comparisons of pollen taxon composition rather than species composition. Human arrival times were derived from the literature and reflect written reports and earliest archeological findings (Table S3).

Chronology

Age-depth models were run for all the island sequences using the Bayesian methodology of Bchron (*39, 40*). This led to chronologies based on the recently updated calibration curves to convert radiocarbon dates into calibrated ages (*41*). IntCal20 is used for sites in the northern hemisphere, and SHCal20 is used for sites in the southern hemisphere. The chronologies of the pollen time-series were transformed into calibrated years before present (cal yr BP; with 1950 CE as the zero level by definition). Radiocarbon (^{14}C) and ^{210}Pb information for each site was provided by the

authors or downloaded from Neotoma. For a few sites, dates were given in pMC (percent Modern Carbon), and these were calibrated beforehand using clam version 2.3.5 (*42*) and region-specific post-bomb curves. We truncated them at 5000 years to permit standardized visualization. The number of iterations in Bchron was set to 100,000; the number of starting iterations was set to 20,000; and the step-size to keep for every iteration beyond the burn-in was set to 80. The age-depth models were run on R version 4.0.2 using the Bchron package version 4.7.2 (*39*, *43*).

Statistical analysis

Data

For each island, the first axis of a Detrended Correspondence Analysis (DCA ordination, R package 'vegan' version 2.5-5 (*44*)) was used to quantify how palynological compositional turnover changed over time before and after human arrival. The metric implicit in DCA is theoretically the optimal metric for analyzing percentage compositional data that contain many zero values (*45*). Similar scores on this ordination axis reflect similar pollen composition. A change in DCA score is interpreted as reflecting a change in pollen composition and hence in vegetation composition. Relating this ordination score to time allows systematic changes in turnover rate to be estimated (*45*). The DCA axis is approximately scaled in standard deviation units of pollen taxon turnover (*45*). A change in axis score of 4 units corresponds roughly to a 100% turnover in the pollen composition of the samples (*45*). While the amount of variation accounted for by the first axis of a DCA ordination varies among datasets, following detailed scrutiny of each ordination we interpreted major changes in DCA axis 1 scores as reflections of human arrival and associated impacts on the vegetation of the island. Because the sign convention in a DCA ordination is arbitrary and for consistency of display, the DCA axis scores were transposed (multiplied by -1) if the sample scores after human arrival were not predominantly positive in DCA space. Subsequent DCA axes were discarded. All analyzes were implemented using R version 4.0.3 (*43*).

Rates of turnover before and after human arrival

To quantify how vegetation turnover (represented by pollen compositional turnover) may have changed with human arrival, we analyzed systematic changes in DCA ordination scores (an indicator of vegetation compositional change) with time using continuous breakpoint models

implemented with standard R syntax lm(y ~ x + {x - breakpoint} * ifelse(x > breakpoint, 1, 0)). These models assume a linear change in composition, allowing rates of turnover to vary between pre- and post-human colonization periods. The slope of the relationship between ordination score (=compositional change) and time indicates the rate of directional turnover (Fig. 1). A paired *t*-test was used to assess significant differences in this slope before and after human arrival (Fig. 2, Table S3). As an additional robustness test, we repeated the breakpoint analysis after randomizing the link between pollen data and time within each record (random order). The median as well as the mean difference in the rate of directional turnover before and after human arrival was always larger in the data when compared to any of 1000 runs on randomized data. Results were visualized using the R package visreg version 2.6-1 (*43*, *46*).

The prescribed breakpoint model was compared with a model including no relationship, as well as a model fitting a linear relationship (Table S5). Explanatory power increases by 32% (median) relative to no-breakpoint linear models when the models prescribe a breakpoint at the date of human arrival (adjusted R^2 values of 0.53 (median) and 0.46±0.26 (mean±SD) for a linear no-breakpoint and 0.70 (median) and 0.65±0.26 (mean±SD) for a human-breakpoint model, Table S3). However, for seven islands, the prescribed breakpoint models do not perform better than linear models without a breakpoint in the rate of directional turnover (ΔAICc>2, 7 out of 27 islands, Table S5). One example is New Caledonia, which in fact shows no linear change but an abrupt shift in pollen composition soon after the estimated time of human arrival (Fig.1). The prescribed-breakpoint linear approach cannot represent this pattern adequately and instead conservatively assumes that there is no change in slope with human arrival on the archipelago. This pattern is better captured by comparing the absolute change in pollen composition with human arrival (Figs. S1 and S2, see next section).

Absolute change in pollen composition with human arrival

The magnitude of absolute changes in pollen composition with human arrival was visualized by comparing the DCA scores before human arrival with those afterwards (Fig. S1). Calculating the distance in DCA scores between the two time periods allows a multi-island assessment of human-induced changes. For each island, we calculated the mean absolute distance between DCA scores before human arrival, the mean absolute distance of all DCA scores after human arrival, as well as

the mean absolute distance between DCA scores before human arrival and DCA scores after human arrival (Fig. S2). Results showed that the distance between pre- to post-human arrival (1.15±0.59; mean±SD) is much larger than the distance between points before human arrival (0.34±0.21) and still twice as large as after human arrival (0.58±0.35).

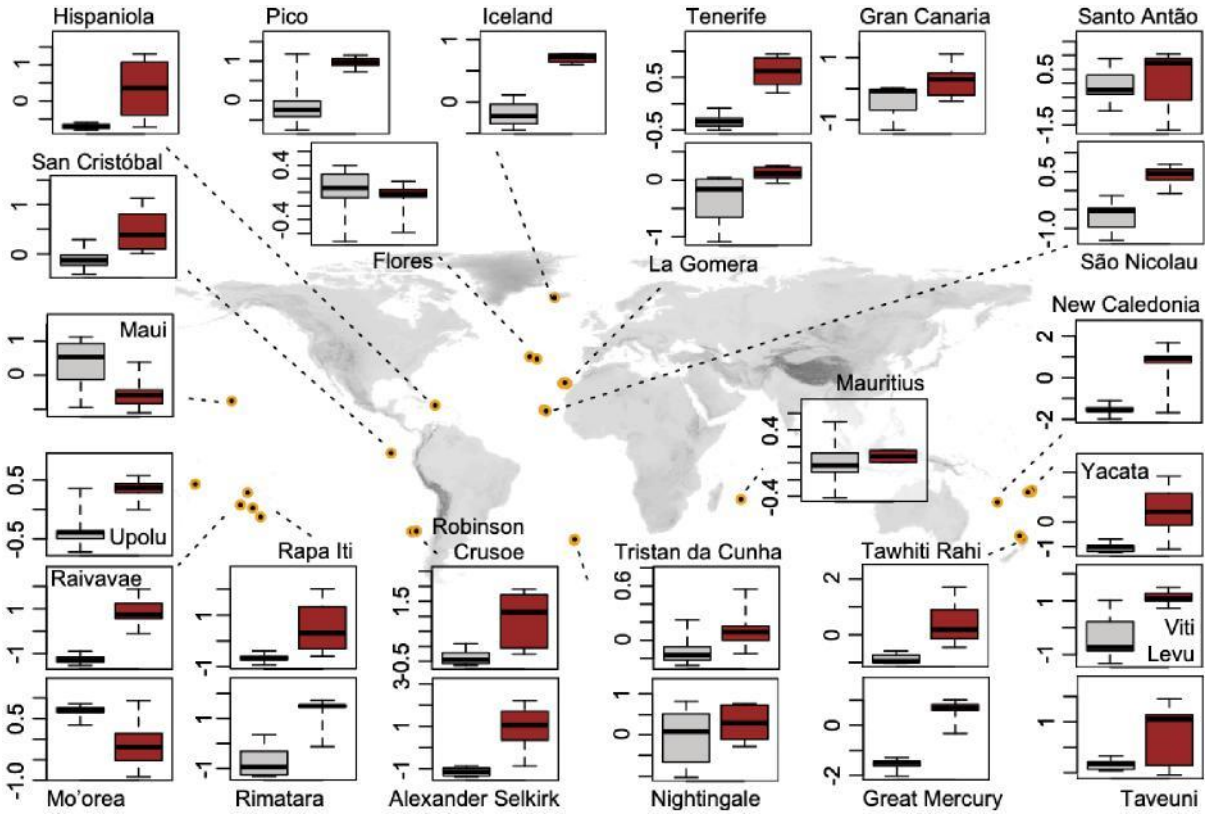

Fig S1: Pollen composition before and after human arrival: Boxplots indicate the DCA axis scores before (grey) and after (red) people arrivals on the different islands. DCA axis scores approximate standard deviations in units of pollen taxon turnover. The difference between the two periods quantifies the magnitude of change (see Fig. S2).

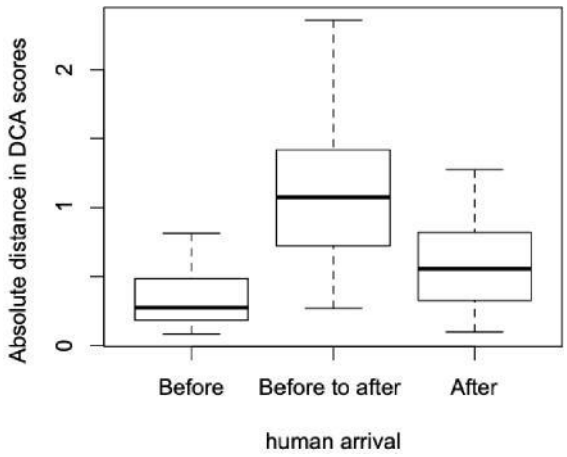

Fig S2: Magnitude of change in pollen composition with human arrival: The distance between DCA axis scores from pre- to post-human arrival (central boxplot) quantifies the absolute change in pollen composition with human arrival (DCA scores approximate standard deviation units of pollen taxon turnover). This distance is much larger than the distance between DCA scores before human arrival (left), or the distance between DCA scores after human arrival (right). Data shown here represent one value for each island (mean distance).

Estimated human arrival time and the onset of vegetation change

Human induced transformation of vegetation composition may sometimes start considerably after (even occasionally before) earliest establishment on the island or earlier than archaeological and historical records attest. We thus implemented a second breakpoint model, which optimizes breakpoint placement based on a likelihood approach using the R package segmented version 1.32 (*47*). An optimal breakpoint that is close to the historically dated arrival of humans based on archaeological and other independent proxy data, indicates that strong human impact starts directly in association with their arrival. A time lag of human impacts would be indicated if the optimal statistically solution lags hundreds of years behind human arrival; a statistically optimal breakpoint preceding the historical arrival point may indicate that humans may have altered the island earlier than indicated by archeological records. It is also possible that non-anthropogenic processes have driven turnover in these situations. The times selected as breakpoints by the model optimization algorithm are within 500 years of the estimated human arrival times in 63% of cases (78% for 1000 years; median difference is 338 years relative to 953 for breakpoint models with randomized data, Table S5). Human arrival estimates lie within the 95% confidence intervals of the optimal breakpoint estimate in 41% of islands.

Quantifying directional rate of change in pollen data with uneven temporal sampling

The aim of the simulations presented below is to test if the ordination-based analytical approach implemented in this study is robust regarding uneven temporal sampling. It shows that the analysis does not suffer from the limitations of traditional rate-of-change quantifications based on bin-by-bin comparisons of directly adjacent stratigraphical levels (*48)*.

Rate-of-change analyzes measure the change in assemblage composition per unit time. Rate-of-change in pollen composition is traditionally quantified by dividing assemblage dissimilarity (i.e. compositional turnover) by the time passed between two adjacent stratigraphical levels (e.g. *48*, *49*). The measured assemblage dissimilarity between these two adjacent stratigraphical levels quantifies long-term directional change as well as random short-term variability. Differentiating directional change from the random variability is impossible while directly comparing two adjacent stratigraphical levels. Equal temporal sampling is necessary if longer time series are analyzed with this approach, as the magnitude of a directional change increases along with temporal distance between two samples, while the effect of random variability remains constant. The need for equal sampling can be bypassed by estimating the entire gradient in the pollen assemblage composition based on all available stratigraphic levels before calculating the rate-of-change. Ordination analyzes have been developed to quantify unknown gradients in assemblage composition with uneven sampling. The directional rate-of-change in assemblage composition can thus be quantified from ordination scores. Analyzing the relationship of the resulting gradient with time provides a powerful tool to measure directional rate-of-change in assemblage composition that is robust with regard to unequal sampling as well as random variability. DCA is particularly suitable for this approach as the units of the first axis measure standard deviations in assemblage composition, with a distance of 4 standard deviations representing complete turnover in composition between samples (*50*). To demonstrate that the rate-of-change estimated using DCA is independent from the temporal distance between samples we implemented two simulation analyses. The simulations implemented below show that this approach works well even with very uneven sampling and high random variability.

Simulation 1: Random sampling along a gradient with length 100 (= 100 timesteps)

A directional gradient in assemblage composition with three species is simulated along a time axis of 100 timesteps. The first species changes its abundance from 1 to 100% along this time axis,

while the second species changes its abundance in the opposing direction from 100 to 1%. A third species is characterized by a constant abundance of 50% along the entire temporal gradient. Simulations were run with and without random variability. Random variability is implemented by adding a random value between -50 and 50 to the abundance of the third species (Fig. S3).

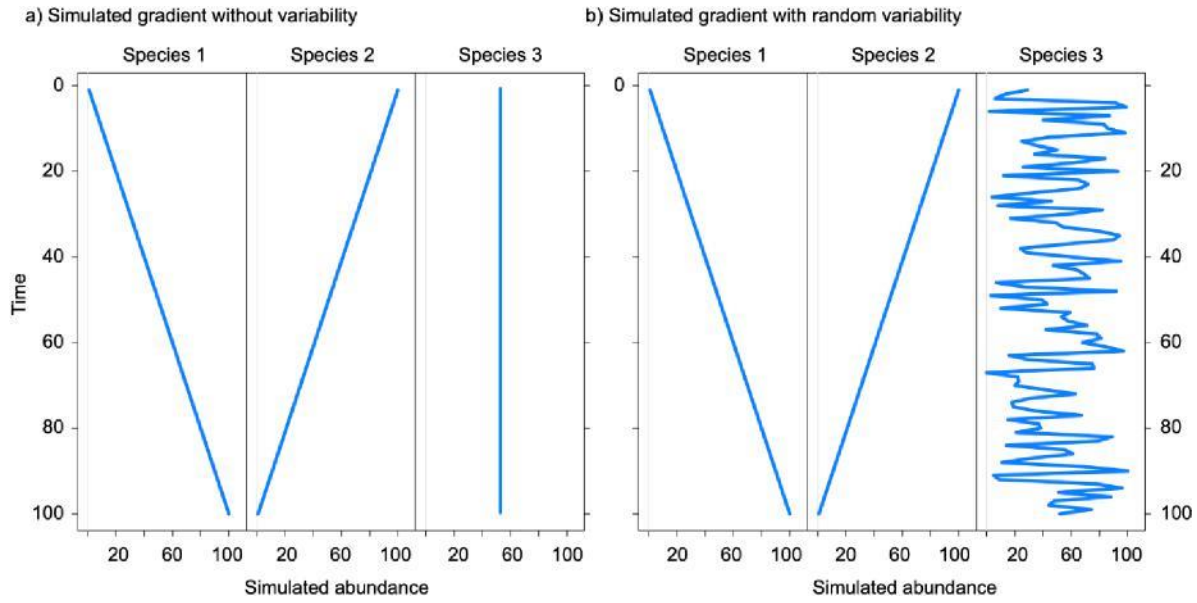

Fig. S3: Simulated gradient in community composition. A directional gradient in species composition was simulated along 100 timesteps with species 1 increasing abundance from 1 to 100%, species 2 decreasing abundance from 100 to 1%. (A) Abundance of species 3 was kept constant at 50% for simulations without variability. (B) Simulations including random variability do so by adding a random value between -50 and 50 to each time step of species 3.

The simulation shows that rate-of-change estimates based on direct comparisons of dissimilarity of adjacent temporal levels is only reasonable without random variability. Equal temporal sampling is needed if the assemblage composition is influenced by random variability.

In the simulated example without variability (Fig. S3A), Chi-square distance between two directly adjacent temporal levels is 0.0162 (per time unit). Increasing the temporal distance to 20 by e.g., comparing stratigraphic level 20 with stratigraphic level 40, results in a dissimilarity of 0.3239 per 20-time units. Further dividing this result by 20 results again in a rate-of-change of 0.0162 per time unit. The rate-of-change estimate is thus independent of the temporal distance between

samples if assemblage composition is only changing along a continuous directional gradient and not influenced by any random variability. Adding variability (Fig. S3B), however, increases dissimilarity between two directly adjacent temporal levels from 0.0162 per time unit (without variability) to 0.3625± 0.0228 per time unit (mean ± standard deviation of 100 independent simulations). Increasing the temporal distance to 20 in the simulation with variability (Fig. S3B) results in a dissimilarity of 0.5085 ± 0.1120 per 20-time units (mean ± standard deviation of 100 runs) or 0.0254 ± 0.0056 per time unit. Random variability that influences assemblage composition independently from the directional gradient thus makes it impossible to compare rate-of-change estimates from time periods that are not sampled with a similar temporal resolution. Uneven temporal sampling will result in non-interpretable results (see Table S1 for an overview).

Table S1: Rate-of-change estimates based on direct comparisons of dissimilarity between adjacent temporal levels implemented for different sampling densities (number of stratigraphic sampling units 100, 50, 20, 10, 5) and strategies (equal distance and random placement) along a simulated temporal gradient of length 100. Analyses were performed for data without random variability (Fig. S3A) and with random variability in assemblage composition (Fig. S3B). Results for the data with random variability represent mean ± standard deviations of 100 independent simulations. Results show a strong effect of random variability on the rate-of-change estimates that further depend on the temporal distance between the sampling units.

Equal sampling

Number of sampling units	**100**	**50**	**20**	**10**	**5**
No variability	0.0162	0.0162	0.0162	0.0162	0.0162
Random variability	0.3625±0.0228	0.1826±0.0187	0.0757±0.0126	0.0412±0.0084	0.0254±0.0056

Random Sampling

No variability	0.0162±0	0.0162±0.0000	0.0162±0.0000	0.0162±0.0000	0.0162±0.0000
Random variability	0.3622±0.0218	0.2511±0.0302	0.1500±0.0381	0.0979±0.0443	0.0622±0.0514

Simulation 2: Detrended correspondence analysis (DCA) approach as implemented in the manuscript

Analyzing rate-of-change with an ordination, in contrast, is able to quantify directional rate-of-change consistently even if stratigraphic levels are sampled unevenly and if random variability in composition is added to the data. DCA quantifies the strongest gradient in assemblage composition

along its first DCA axis. Each pollen assemblage in a stratigraphic level receives a coordinate on that axis (axis score). Differences in axis scores between two pollen assemblages are proportional to changes in assemblage composition and proportional to standard deviations (SD). A change in axis score of 4 SD units corresponds roughly to a 100% turnover in the pollen composition. Relating axis scores of the first DCA with time using linear regression allows estimation of the directional rate-of-change along the gradient in assemblage composition identified by the DCA. An additional important feature of DCA is that the transformations implicit in the dissimilarity metric used in DCA provides a solution to the problem of analyzing numerically closed percentage data that contain many zero values, such as pollen data (*50*).

When we implemented this methodology in the simulation analysis, we found that the simulated example without variability (Fig. S3A) had a rate of change of 0.0142 SD_{ptt} (directional change in composition measured in standard deviations of pollen assemblage turnover (SD_{ptt}) per time unit) (Table S2). Increasing the temporal distance to 20 (5 equally spaced samples along 100-time units) results in a very similar rate-of change estimate (0.0141 SD_{ptt}, Table S5, Fig. S4A). The rate-of-change estimate is thus independent of the temporal distance between samples. Adding random variability (Fig. S4B) results in very similar rate-of-change estimates with 0.0142±0.0003 SD_{ptt} for 100 equally spaced samples (Fig. S3B). The estimate is even robust if only 5 unevenly distributed samples are taken along the entire gradient (0.0145±0.0027 SD_{ptt}, Table S2). Estimates of directional rate-of-change are thus highly robust with respect to uneven sampling and random variability (Table S2, Fig. S4).

Table S2: Rate-of-change estimates via Detrended Correspondence Analysis (DCA) implemented for different sampling densities (number of sampled stratigraphic levels 100, 50, 20, 10, 5) and sampling strategies (equal distance and random placement) along a simulated temporal gradient of length 100. Analyses were performed for data without random variability (Fig. S3A) and with random variability in assemblage composition (Fig. S3B). Results for the data with random variability represent mean ± standard deviations of 100 independent simulations. Results show that rate-of-change estimates (via DCA) are independent of the distance between sampled units and are not systematically affected by random variability in assemblage composition. The methodology is thus suitable to quantify directional rate-of-change in pollen data.

Equal sampling

Number of sampling units	**100**	**50**	**20**	**10**	**5**
No variability	0.0142	0.0142	0.0142	0.0141	0.0141
Random variability	0.0142±0.0003	0.0141±0.0004	0.0141±0.0007	0.0143±0.0011	0.0143±0.0016

Random Sampling

No variability	0.0142±0	0.0142±0.0001	0.0141±0.0001	0.0140±0.0002	0.0141±0.0004
Random variability	0.0142±0.0003	0.0141±0.0004	0.0141±0.0008	0.0141±0.0012	0.0145±0.0027

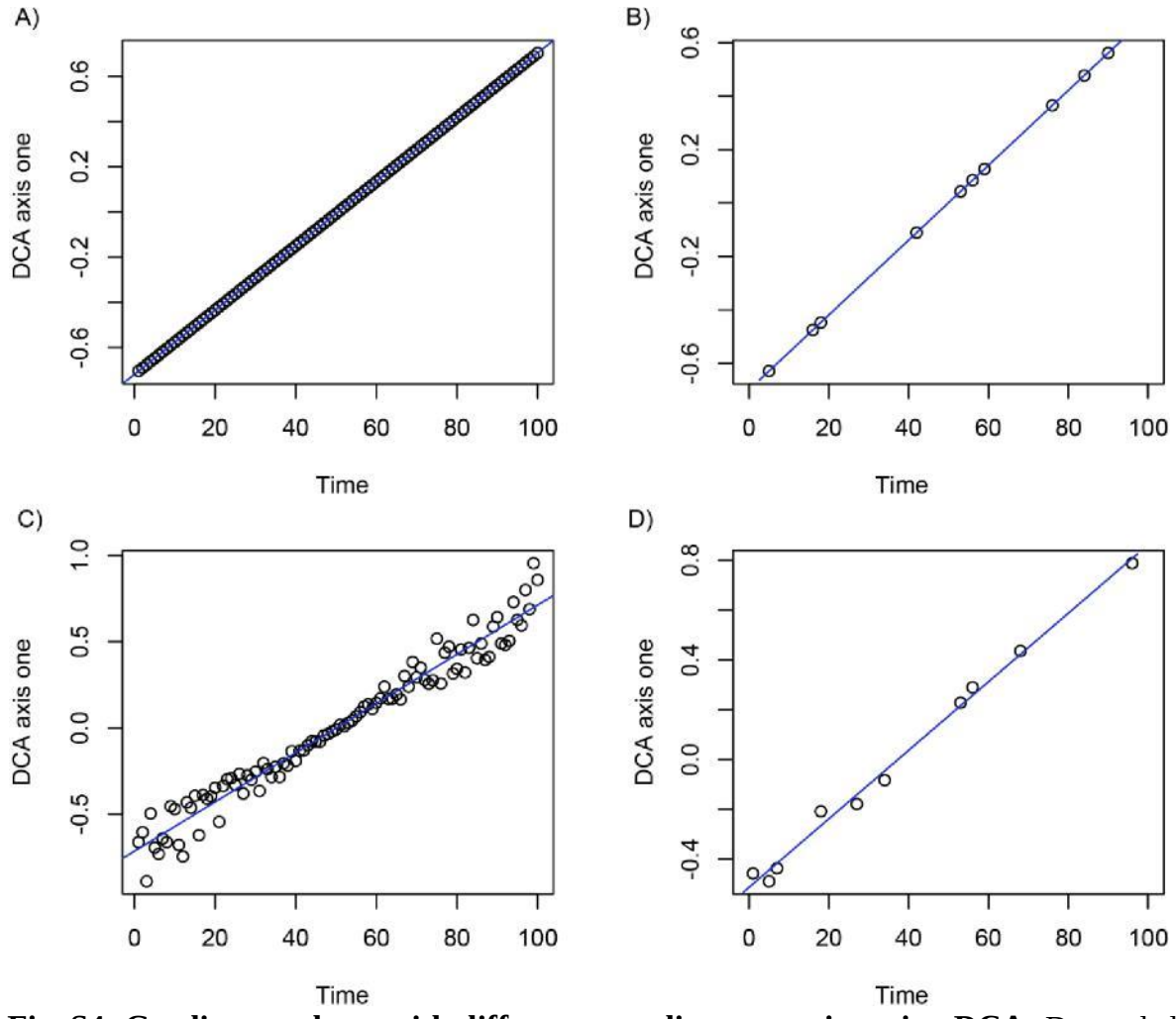

Fig. S4: Gradient analyses with different sampling strategies using DCA: Detrended correspondence analyses (DCA) order the major gradient in assemblage composition along the first axis. Rate-of-change is quantified as the slope of the regression between the scores of this first DCA-axis with time (blue lines). This slope is constant and independent of the sampling strategy (even sampling in A and C; uneven sampling in B and D) as well as the amount of random variability (no variability in A and B; with random variability in C and D).

Analyzing possible influences of geographic covariables on the magnitude of human effects. Human arrival affects vegetation turnover considerably, but the magnitude differs between islands. The diversity of the analyzed islands allows us to test whether this difference in the effect of human arrival can be explained by the timing of when humans entered the island system or by present and past geo-environmental characteristics of the islands. Analyses were conducted with linear models explaining the difference in pre- and post-human arrival turnover. Explanatory variables include the timing of human arrival as well as current and historic geographic characteristics (Table S3 and Box1).

Box S1: Explanatory variables included in Figure 3 and their potential function.

Variable	Function
Human arrival time	The purpose (e.g. exploitation or settlement) and toolkit available to humans to modify pristine islands after arrival changes with time (e.g. *51*). For example, there are studies referring to early impacts on ecological systems as 'first contact extinctions' (e.g. *52*).
Latitude (º)	Ecological systems (*53*) and cultural diversity (*54*) are known to differ with latitude, which may change the effect human actions have when arriving in pristine ecosystems.
Elevation (m a.s.l.):	Elevation where the sedimentary sequence was collected may have an effect on vegetation turnover. Lower elevations might be more accessible to humans and thus more impacted than higher elevation island ecosystems (*55*).
Island area (km^2)	Smaller islands may show a greater rate of vegetation turnover than bigger islands and generally support fewer stable populations (*56, 57*). In addition, island resources are more limited. These characteristics may translate into a stronger human impact.
Glacial-interglacial island area (km^2)	Variations in island area over time account for the legacy effect of past sea-level change (*35, 58*). We used the median sea-level (as calculated over the previous nine glacial cycles) following *35*.
Isolation quantified by: distance of island to mainland (km) and surrounding landmass (km^2)	Quantified as direct distance as well as the proportion of surrounding landmass (*59*). More isolated islands tend to have been inhabited by people more recently and therefore island taxa are more susceptible to human arrivals.
Absolute rate of turnover before human arrival	To test how the natural rates of vegetation turnover in pre-human times may affect early human impacts (*51, 52,* 60).

Table S3. Human arrival times and geographic characteristics for the islands studied

Islands used in this study organized by ocean. Island area depicts the current situation as well as long-term median over the previous nine glacial-interglacial cycles (*35, 58*). Isolation was estimated using distance from the mainland as well as the proportion of surrounding landmass (*SLMP*) (*59*). Human arrival times were extracted from original data sources. Cal yr BP ages use 1950 CE as the zero level. Notes: [h]Debated pre-Portuguese arrivals to the Azores; [hh]First migration of agriculturalist societies in Hispaniola; [hhh]Portuguese arrival in 1506 CE, while the first regular settlement on Tristan da Cunha was established between 1810 and 1820 CE; [hv]European arrival on San Cristóbal was in 1535 CE, with the introductions of goats occurring in 1813-1835 CE, while the first regular settlement on San Cristóbal was established between 1842 and 1845 CE.

Ocean	Archipelago	Island	Latitude, Longitude (°)	Core elevation (m a.s.l)	Island area (km²; current and long-term)	Distance [km]	SLMP [km²]	Human arrival (cal yr BP)	References for human arrival
Atlantic	Azores	Flores	39.41, -31.22	530	143, 217	1872	0.44	468[h]	*[61, 62]*
	Azores	Pico	38.44, -28.20	903	447, 487	1637	0.46	468[h]	*[61, 62]*
	Cabo Verde	São Nicolau	16.62, -24.35	1000	388, 445	750	0.46	370	*[63]*
	Cabo Verde	Santo Antão	17.11, -25.06	1200	785, 944	857	0.42	370	*[63]*
	Canary Islands	Gran Canaria	28.03, -15.33	870	1560, 2183	220	0.81	2000	*[64, 65]*
	Canary Islands	La Gomera	28.07, -17.15	1250	370, 518	347	0.76	1800	*[65, 66]*
	Canary Islands	Tenerife	28.30, -16.19	600	2034, 2381	310	0.76	2000	*[65, 67]*
	Greater Antilles	Hispaniola	19.03, -70.92	2455	76480, 84232	715	0.37	2500[hh]	*[68]*
	Tristan da Cunha	Nightingale Island	-37.4, -12.5	180	3, 25	2795	0.27	444[hhh]	*[69]*
	Tristan da Cunha	Tristan da Cunha	-37.0, -12.3	63	98, 133	2777	0.27	444[hhh]	*[69]*
	Mascarenes	Mauritius	64.02, -20.71	80	102775, 126840	1209	0.61	1076	*[70]*
	Fiji	Taveuni	-20.40, 57.52	530	2040, 2670	1874	0.40	302	*[71]*
	Fiji	Viti Levu	-16.83, -179.94	810	442, na	2963	0.30	3000	*[72]*
	Fiji	Yacata	-18.07, -178.53	4	10531, 21769	2707	0.21	3000	*[72, 73]*
	Galápagos	San Cristóbal	-0.89, -89.48	679	558, 803	948	0.24	115[hv]	*[74, 75]*
	Hawaiian Islands	Maui	20.79, -156.47	0	1884, 3004	3706	0.29	750	*[76]*
	Juan Fernández Islands	Alexander Selkirk	-33.75, -80.83	1200	50, 54	752	0.26	385	*[77]*
	Juan Fernández Islands	Robinson Crusoe	-33.60, -78.90	130	48, 118	609	0.34	385	*[77]*
	New Caledonia	Grande Terre	-22.27, 166.61	3	18576, 38254	1354	0.17	2800	*[72]*
	Mercury Islands	Great Mercury	-36.61, 175.79	5	20, 155458	2179	0.39	780	*[78]*
	Poor Knights	Tawhiti Rahi	-35.47, 174.73	50	2, 6	2070	0.45	780	*[19]*
	Sāmoa	Upolu	-13.9, -171.83	760	1125, 1786	3887	0.22	2800	*[72, 79]*
	Society Islands	Mo'orea	-17.5, -149.83	83	133, 165	5868	0.24	1000	*[80, 81]*
	Austral Islands	Rimatara	-22.64, -152.81	5	9, 10	5500	0.20	750	*[81]*
	Austral Islands	Raivavae	-23.87, -147.68	1	18, 105	5830	0.20	750	*[81]*
	Austral Islands	Rapa Iti	-27.60, -144.35	2	38, 95	6010	0.19	750	*[81]*

Table S4. Data sources for island palaeoecological records included in Figure 1. The Neotoma Paleoecology Database is available at www.neotomadb.org (*105*, *106*).

Ocean	Archipelago	Island	Data source	Reference
Atlantic	Azores	Flores	S.E. Connor	*(3)*
Atlantic	Azores	Pico	S.E. Connor *et al.*	*(3, 82)*
Atlantic	Cabo Verde	São Nicolau	A. Castilla-Beltrán & S. Nogué	*(83)*
Atlantic	Cabo Verde	Santo Antão	A. Castilla-Beltrán & S. Nogué	*(84)*
Atlantic	Canary Islands	Gran Canaria	L. de Nascimento	*(85)*
Atlantic	Canary Islands	La Gomera	S. Nogué	*(29)*
Atlantic	Canary Islands	Tenerife	L. de Nascimento	*(86)*
Atlantic	Greater Antilles	Hispaniola	Neotoma	*(87)*
Atlantic	Tristan da Cunha	Nightingale Island	K. Ljung & S. Björck	*(88)*
Atlantic	Tristan da Cunha	Tristan da Cunha	K. Ljung & S. Björck	*(89)*
Atlantic	Iceland	Iceland	Neotoma	*(90)*
Indian	Mascarenes	Mauritius	Neotoma & E.J. de Boer	*(91)*
Pacific	Fiji	Taveuni	J. Stevenson & M. Prebble	*(92, 93)*
Pacific	Fiji	Viti Levu	Neotoma & J. Stevenson	*(93)*
Pacific	Fiji	Yacata	J. Stevenson	*(93)*
Pacific	Galápagos	San Cristóbal	Neotoma	*(26)*
Pacific	Hawaiian Islands	Maui	Neotoma	*(94)*
Pacific	Juan Fernández Islands	Alexander Selkirk	S.G. Haberle	*(95)*
Pacific	Juan Fernández Islands	Robinson Crusoe	S.G. Haberle	*(96, 97)*
Pacific	New Caledonia	Grande Terre	J. Stevenson	*(27)*
Pacific	Mercury Islands	Great Mercury	Neotoma & M. Prebble	*(98, 99)*
Pacific	Poor Knights	Tawhiti Rahi	J.M. Wilmshurst	*(19)*
Pacific	Sāmoa	Upolu	W.D. Gosling *et al.*	*(18)*
Pacific	Society Islands	Mo'orea	J. Stevenson	*(100)*
Pacific	Austral Islands	Rimatara	M. Prebble	*(101)*
Pacific	Austral Islands	Raivavae	Neotoma & M. Prebble	*(99)*
Pacific	Austral Islands	Rapa Iti	Neotoma & M. Prebble	*(99, 102, 103)*

Background information on the impacts of climate change and volcanic eruptions for the islands included in Tables S3 and S4

Vegetation turnover is not only linked to human activities but also to many other disturbances including volcanic activities, climate change, extreme weather events, fire, and sea-level fluctuations. While those factors influence vegetation composition, they cannot explain the systematic change in turnover that we attribute to human arrival over the analyzed time period.

When looking at the islands independently, the original authors found no evidence of lasting changes in local vegetation assemblage caused by past climate change over the studied time period of the past 5000 years. For example, on Galápagos fluctuating shifts in vegetation abundance were found in response to El Niño/La Niña with a reversion to the previous state following climatic oscillations (*26*). For the other Pacific islands (e.g. *18, 26, 27, 92-97*, *100-103*) included in this study, such as Tawhiti Rahi (*19*) and Great Mercury (*98, 99*), there are no reliable data pinpointing major vegetation responses to specific climatic events for the past 2000 years (but see *104*). In the Azores, there was a weak link between vegetation and paleoclimatic changes detected through geochemical proxies on the island of Pico. Even if the Azorean paleoclimate varied substantially (e.g. cooler/drier periods occurred 400–800, 1300–1800, 2600–3000, 3300–3400 and possibly also 4400–4600 cal yr BP) its impact on the local vegetation, at least in terms of pollen composition, was relatively small (*3*). On La Gomera (Canary Islands), there was a decline in hygrophilous plant taxa towards the present, possibly linked to the end of a regional climatic change called the African Humid Period (5000 years ago) (*29, 107*). However, on the other Canary Islands (Tenerife and Gran Canaria) (*85, 86*) and Cabo Verde (Santo Antão and São Nicolau) (*83, 84*), the age of the sedimentary sequences was not old enough to detect potential changes related specifically to this regional climatic change. Further south in the Atlantic Ocean, on Tristan da Cunha, paleoecological studies show a local dry period (1050–1450 cal yr BP) assocated with an increase in sedges (*89*). On Nightingale Island there were recurrent humid periods during the Holocene. The most recent of these dated back to 1800–2600 cal yr BP and 4700 cal yr BP. These seem to have had mostly local effects on the vegetation (*88*), with a return to prior vegetation composition after humidity decreased. Climate in the southwest Indian Ocean is mainly controlled by the monsoon system at orbital and millennial timescales. Most studies use isotope data from stalagmites to reconstruct hydroclimate variability. A study from Rodrigues Islands (*108*) located 560 km east of Mauritius shows a recurring submillennial-scale aridity trend punctuated by multidecadal megadroughts throughout the past 8000 years. This suggests that the insular fauna and flora in the Mascarenes survived prior episodes of severe climate stress on the islands, but collapsed when a substantial increase in human activities started, which coincided with the late Holocene drying trend (*91, 109*). In summary, these data provide strong evidence of "pre-human island systems" that responded to climatic forcing but were capable of shifting back to their prior state.

The volcanic eruptions found in sedimentary sequences are inferred from chronologically dated tephra layers. However, most of the island sites do not have an independent study on tephrochronology and the tephra layers are not all well-dated. Hence, the quality of the information might be skewed between islands. In addition, individual volcanic eruptions typically are short-lived perturbations to the climate system, with effects lasting on the order of 1-3 years. These short time-periods are considered to be too brief to explain the trends seen here. Taking into account these limitations, when reviewing the original datasets for each island we found minimal vegetation responses to volcanic eruptions. In New Zealand if we looked at vegetation responses to the eruption of the Okataina volcano (600 cal yr BP), the authors found only minor disturbance, where tephra layers were found in most places in northern New Zealand, suggesting that the signature of human settlement overwhelmed the signature of this eruption (*19, 109, 110*). There are no known eruptions that affected Rimatara, Raivavae, or Rapa Iti. In the Azores, volcanic eruptions appear to have had localized impacts on the vegetation, lasting 500–1000 years and favoring endemic taxa (*3*). The main impacts seem to have occurred in the last 2000 years on Pico (the Caveiro pollen record (*82*)), with temporary declines in arboreal pollen every time there was an eruption (*3, 82*). On Nightingale Island, where a tephra layer was identified (dated to around 3400 cal yr BP), the authors do not find any significant change in vegetation that could be directly linked to this eruption (*88*). On Tristan da Cunha, numerous small eruptions have been recorded during the Holocene as, for example, the tephra layer found at around 500–700 cal yr BP (*89*). If there were any vegetation effects on this island associated with these eruptions, they were too small to be recorded by the pollen data (*86*). The same explanation is suggested for the Canary Islands (29, *85, 86*) and Cabo Verde (*83, 84*). In Mauritius, the last volcanic activity was dated at 25,000 years ago (*111*). Since then, the hotspot of volcanic activity has moved towards the southwest and is currently located off the southeast coast of Réunion. The *Piton de la Fournaise* is a highly active volcano, but there are neither historical eruptions nor other indications that pre-historic volcanic activity to have directly impacted the other Mascarene islands (*91*).

Table S5. Breakpoint model results by island

Summary statistics (AICc and adjusted R^2) for the four implemented breakpoint models relating DCA ordination scores (SDptt, standard deviation of pollen taxon turnover = compositional change) with time. Implemented models include no relationship (no slope), a linear relationship with no breakpoint (linear), a linear breakpoint model with estimated human arrival time as a prescribed breakpoint (prescribed), as well as a linear breakpoint model with optimized breakpoint (optimal). Bold text indicated the no-slope, linear, or human breakpoint model is considered best (AICc difference >2 to the less complex model). Asterisks (*) indicate two islands (Grande Terre and Rimatara) where turnover shifted abruptly with human arrival. Such a jump in composition is a clear indication of human effects that our modelling approach will treat conservatively as no change in turnover. The two "slope" columns depict the slope (change in ordination score with time) of the human breakpoint model before and after human arrival (SDptt/100 years). The right column depicts the percentage of inertia (weighted variance) explained by the first DCA axis relative to the total inertia of a correspondence analysis.

Island	AICc				Adjusted R_2			Breakpoint		Slope		DCA
	no slope	**linear**	**prescribed**	**optimal**	**linear**	**prescribed**	**optimal**	**prescribed**	**optimal**	**before human**	**after human**	**% expl.**
Flores	9.5	-3.0	-11.3	-10.4	0.26	0.41	0.43	468	343	-0.030	0.047	40
Pico	145.0	125.0	100.8	45.4	0.22	0.41	0.70	468	984	0.011	0.256	46
São Nicolau	51.0	47.1	30.4	43.7	0.18	0.58	0.39	370	235	0.005	0.267	25
Santo Antão	88.9	86.6	77.7	72.4	0.08	0.27	0.39	370	109	-0.013	0.280	23
Gran Canaria	44.1	20.3	17.5	18.5	0.65	0.71	0.74	2000	1839	0.048	0.147	23
La Gomera	15.1	-3.2	-4.7	-24.2	0.59	0.65	0.88	1800	3629	0.030	0.001	21
Tenerife	43.2	14.5	-11.6	-27.0	0.66	0.87	0.93	2000	2411	0.013	0.120	42
Hispaniola	86.8	45.4	1.1	-39.3	0.71	0.92	0.98	2500	1435	-0.017	0.084	48
Nightingale	74.9	68.3	70.5	71.3	0.18	0.17	0.20	444	2655	0.020	-0.029	40
Island Tristan	18.6	7.0	-16.3	-27.8	0.33	0.69	0.80	444	3	-0.013	0.144	56
da Cunha	23.6	5.1	4.4	4.4	0.66	0.70	0.76	1076	1677	0.015	0.063	47
Iceland	-12.5	-30.5	-54.3	-45.5	0.31	0.57	0.52	302	2424	0.005	0.213	13
Mauritius	79.3	60.9	50.4	52.9	0.53	0.71	0.72	3000	2775	-0.034	0.090	31
Taveuni Viti	65.4	45.6	35.2	30.8	0.61	0.77	0.83	3000	3806	0.148	-0.019	29
Levu Yacata	82.0	41.4	22.6	25.1	0.79	0.90	0.90	3000	2814	-0.002	0.104	27
San Cristóbal	104.7	-21.5	-303.2	-339.7	0.40	0.81	0.83	115	65	0.013	0.544	25
Maui	79.6	81.5	83.4	79.8	-0.01	-0.03	0.15	750	1599	-0.005	-0.066	22
Alexander	85.8	67.6	58.6	61.7	0.55	0.70	0.70	385	379	0.020	0.664	22
Selkirk Robinson	51.5	53.0	3.2	6.7	0.01	0.93	0.93	385	381	-0.013	1.488	61
Crusoe Grande	89.9	52.2*	54.6	51.0	0.78	0.77	0.82	2800	622	0.053	0.077	26
Terre Great	84.8	52.9	18.9	13.6	0.71	0.92	0.94	780	1109	0.023	0.295	31
Mercury Tawhiti	59.4	24.5	1.6	4.9	0.80	0.93	0.93	780	767	0.035	0.236	24
Rahi Upolu	28.6	9.8	12.7	14.8	0.61	0.59	0.61	2800	4075	0.019	0.026	37
Mo'orea	102.1	96.1	86.9	80.2	0.11	0.25	0.35	1000	838	-0.302	0.005	24
Rimatara	98.2	80.2	67.8*	52.3	0.48	0.67	0.82	750	1199	0.012	0.407	35
Raivavae Rapa	86.7	25.6	26.6	15.2	0.90	0.90	0.94	750	1088	0.195	0.285	40
Iti	68.6	58.3	17.4	19.9	0.38	0.89	0.89	750	693	-0.004	0.287	26